# $NOHSO_4$/HF – A Novel Etching System for Crystalline Silicon

Sebastian Patzig[a], Gerhard Roewer[a], Edwin Kroke[a], and Ingo Röver[b]

[a] TU Bergakademie Freiberg, Department of Inorganic Chemistry, Leipziger Straße 29, D-09596 Freiberg, Germany
[b] Deutsche Solar AG, Solar Materials, Alfred-Lange Straße 18, D-09599 Freiberg, Germany

Reprint requests to Prof. Dr. E. Kroke. E-mail: kroke@chemie.tu-freiberg.de

*Z. Naturforsch.* **2007**, *62b,* 1411 – 1421; received June 12, 2007

Solutions consisting of HF – $NOHSO_4$ – $H_2SO_4$ exhibit a strong reactivity towards crystalline silicon which is controlled by the concentrations of the reactive species HF and $NO^+$. Selective isotropic and anisotropic wet chemical etching with these solutions allows to generate a wide range of silicon surface morphology patterns. Traces of $Ag^+$ ions stimulate the reactivity and lead to the formation of planarized (polished) silicon surfaces. Analyses of the silicon surface, the etching solution and the gas phase were performed with scanning electron microscopy (SEM), DR/FT-IR (diffusive reflection Fourier transform infra-red), FT-IR, Raman and NMR spectroscopy, respectively. It was found that the resulting silicon surface is hydrogen-terminated. The gas phase contains predominantly $SiF_4$, NO and $N_2O$. Furthermore, $NH_4^+$ is produced in solution. The study has confirmed the crucial role of nitrosyl ions for isotropic wet chemical etching processes. The novel etching system is proposed as an effective new way for selective surface texturing of multi- and monocrystalline silicon. A high etching bath service lifetime, besides a low contamination of the etching solution with reaction products, provides ecological and economical advantages for the semiconductor and solar industry.

*Key words:* Acidic Etching, Mono- and Multicrystalline Silicon, Nitrosyl Ion

## Introduction

Wet chemical etching of crystalline silicon is widely used in the semiconductor and the photovoltaic industry. The applications of conventional HF – $HNO_3$ – $H_2O$ mixtures for saw damage removal, decoration of surface defects, texturing of silicon surfaces as well as for the recycling of used solar modules have attained enormous economical significance [1, 2]. Another example requiring highly selective etching solutions is the recently discovered formation of "Rolled-Up Nanotubes" (RUNT) [3], a very interesting and promising processing technique for semiconductor nanostructures. Exhausted industrial etching solutions contain high amounts of nitrogen oxides which together with different silicon species require expensive disposal measures. Thus, it is highly important to look for alternative etching solutions which are more selective, more easy to recycle and have longer bath service lifetimes. The wet chemical silicon etching process consists of two reactions taking place simultaneously: The stepwise oxidation of the surface silicon atoms by an oxidizing agent, which itself is reduced to reduction products, and the formation of water soluble complexes by a complexing agent.

For the conventional isotropic etching system Si/HF – $HNO_3$ – $H_2O$ Robbins and Schwartz have proposed that the oxidation by $HNO_3$ might lead to the intermediate formation of $SiO_2$, followed by the cleavage of the Si–O bonds by HF and the consecutive formation of water soluble complexes ($H_2SiF_6$) [4].

The mechanism of dissolution of crystalline silicon by conventional etching mixtures is under intensive investigation. Several steps, concerning in particular the role of the reduction products of nitric acid ($NO_2$, NO, $N_2O_3$, $HNO_2$) acting as oxidizing agents have been postulated [5 – 10]. Because of the complex chemical situation and numerous diffusion and adsorption processes at the surface/solution interface a consistent mechanistic proposal is still missing [4, 11 – 13]. Recapitulating, silicon oxidation and complexation provide the thermodynamic momentum, while sterical hindrance and interactions of charged (+/–) surface sites control the attack of the surface silicon atom and determine the kinetics of the overall etching process [14 – 17].

0932–0776 / 07 / 1100–1411 $ 06.00 

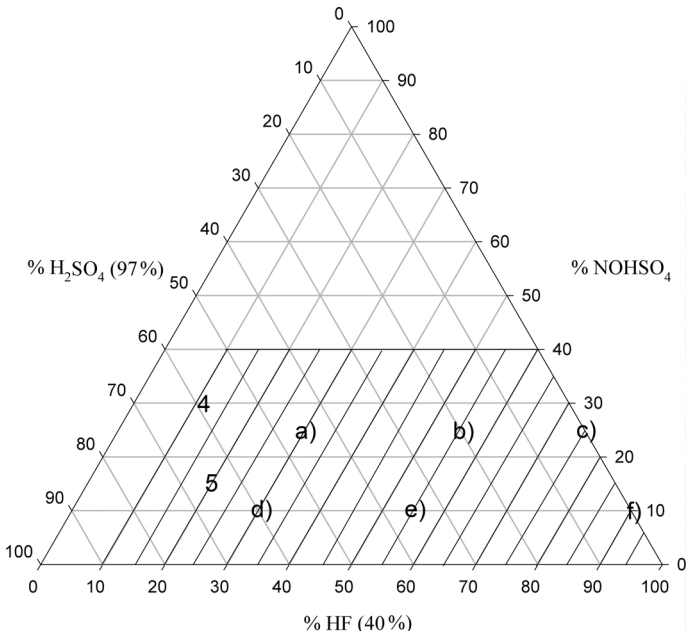


Fig. 1. Pseudo-ternary phase diagram of the $NO^+$-based etching system HF (40 %) – $NOHSO_4$ – $H_2SO_4$ (97 %). The letters a – f and numbers 4 and 5 refer to the SEM images in Fig. 3 a – f, 4 and 5, respectively.

For pH values lower than the isoelectric point of the silicon surface ($pH < pH_{iso}$ (Si–O–Si) = 1.8 – 2.0) solvated anions arrange themselves along the positively charged surface due to Coulomb forces ($F^-$, $SiF_6^{2-}$, $H_2O$) [18, 19]. In order to attack the silicon surface, reactants of the etching solution have to penetrate the negatively charged "wall". Thus, for negatively charged species the activation barrier is much higher than for cations. Therefore, it seems unlikely that the nitrate ion is the real oxidizing species in the classical etching system. However, nitric acid is protonated in highly acidic solutions and dissociates according to Eq. 1. This reaction provides positively charged nitryl ions ($NO_2^+$) which should be able to pass easily the negatively charged barrier and act as oxidizing agents for the surface silicon atoms [20].

$$HNO_3 + H^+ \rightleftarrows H_2NO_3^+ \rightleftarrows H_2O + NO_2^+ \quad (1)$$

The patented use of $NaNO_2$ as a "catalyst" has been known for a long time, but a satisfactory explanation for the reactivity enhancement towards crystalline silicon has not yet been presented [4]. The dissociation of $NaNO_2$ and subsequent protonation of $NO_2^-$ in highly acidic solution should lead to the formation of nitritacidium ions ($H_2NO_2^+$) and finally to nitrosyl ions ($NO^+$) (Eq. 2 and Eq. 3), acting as oxidizing agent for the surface silicon atoms [21].

$$NaNO_2 + H_3O^+ \rightleftarrows Na^+ + HNO_2 + H_2O \quad (2)$$

$$HNO_2 + H^+ \rightleftarrows H_2NO_2^+ \rightleftarrows NO^+ + H_2O \quad (3)$$

This paper is devoted to the development of an alternative silicon etching system by successive replacement of components in the conventional etching system Si/HF – $HNO_3$ – $H_2O$. The oxidizing agent nitric acid is substituted by nitrosyl hydrogensulphate ($NO^+HSO_4^-$), its crucial role and the underlying reduction pathway for the overall etching process are discussed. Aspects of improved control over the etching results, the reactivity towards crystalline silicon, selective silicon surface texturing, increased bath service lifetime, and lower toxicity of waste solutions and gaseous products are considered.

The etching solution was characterized by Raman and NMR spectroscopy, while the gas phase was investigated by means of IR spectroscopy. Analysis of the etched silicon surface was performed by DR/FT-IR spectroscopy and the obtained surface morphologies for multi- and monocrystalline silicon wafers were investigated by SEM.

## Results and Discussion

### *Selection of the etching solution*

Due to the instability of the nitrosyl ions in etching mixtures with high water content, concentrated sulphuric acid (97 % $H_2SO_4$) is the solvent of choice. It binds the water of hydrofluoric acid (40 % HF)

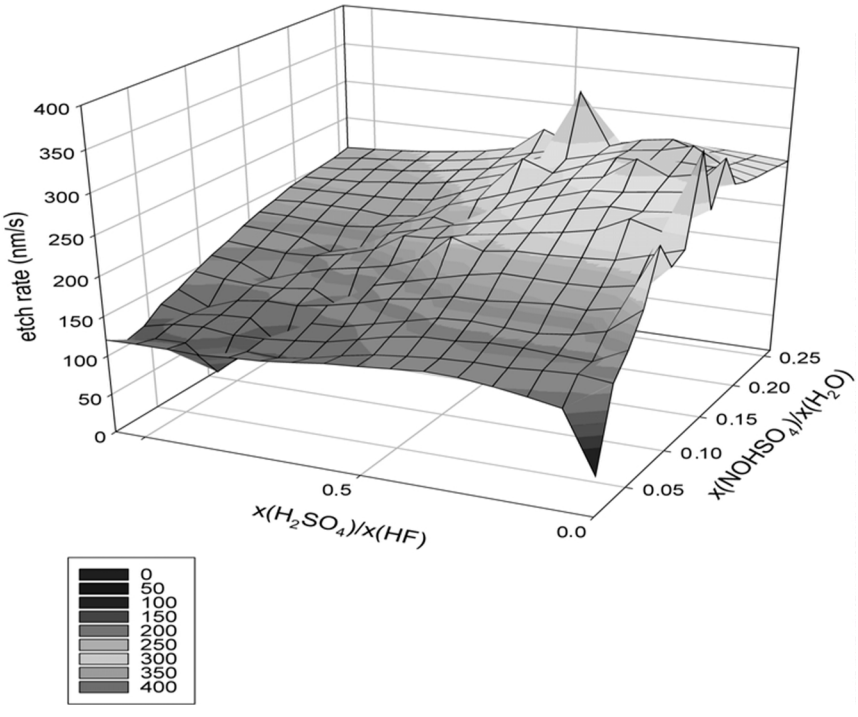


Fig. 2. Etching rate *vs.* mole fraction ratios for the reaction of monocrystalline silicon with novel etching mixtures (600 s etching time). The mole fractions $x$ represent the dissolved species, the water contents of the concentrated acids [HF (40 %) and $H_2SO_4$ (97 %)] are totalized as $x(H_2O)$.

and has been reported as a suitable solvent for $NO^+HSO_4^-$ [22]. The concentration ratio of the etching mixtures was varied in the HF-rich region of the ternary HF (40 %) – $NOHSO_4$ – $H_2SO_4$ (97 %) system. The results of this systematic reactivity and etching morphology studies are presented and discussed in the following section.

*Results of the etching process: etching rates and surface morphologies*

The pseudo-ternary plot shown in Fig. 1 indicates the investigated composition range of the etching solution (striped pattern). It can be derived that hydrofluoric acid was present in excess with respect to the nitrosyl ion concentration.

The etching mixture exhibits a high reactivity towards mono- and multicrystalline silicon. The maximum etching rate achievable is in the range of 350 nm $s^{-1}$, as compared to several hundred up to 3000 nm $s^{-1}$ for mixtures with nitric acid. The results of systematic reactivity studies for monocrystalline silicon are presented in Fig. 2.

The etching rates and surface morphologies can be controlled by (i) the nitrosyl ion concentration and (ii) the $H_2SO_4$/HF ratio, respectively. A low water content in combination with $(H_2SO_4)/(HF)$ ratios in the range of 0.25 – 0.50 provides the conditions for the highest etching rates. The maximum etching rate of $r$ = 350 nm/s has been found for $x(NOHSO_4)/x(H_2O)$ = 0.23 and $x(H_2SO_4)/x(HF)$ = 0.45. High nitrosyl ion concentrations enhance the etching rate by stimulation of oxidation steps and lead to extensive surface ablation. Variation of the concentration ratios offers a broad range of etching figures, which includes isotropic and anisotropic surface structures. This illustrates the versatile modes of application of the novel etching system and the complex relations of etching mixture compositions and the resulting structures of monocrystalline silicon surfaces (Figs. 3 a – f).

The high redox potential of $NO^+/NO$ ($E^\circ$ = 1.45 V *vs.* NHE) facilitates rapid oxidation of surface silicon atoms by injection of holes in the valence band [23], in particular for homogeneous surface covering. Hence, diffusion of the complexing agent (HF) to and away from the silicon surface might become more rate determining. Local variations of the surface reactivity due to inhomogeneous charge density and sterical barriers of surface sites are levelled off. Consequently, anodic and cathodic surface reactions proceed uniformly and isotropic (plained/polished) silicon surfaces are produced, indicating isotropic etching reactions (Figs. 3

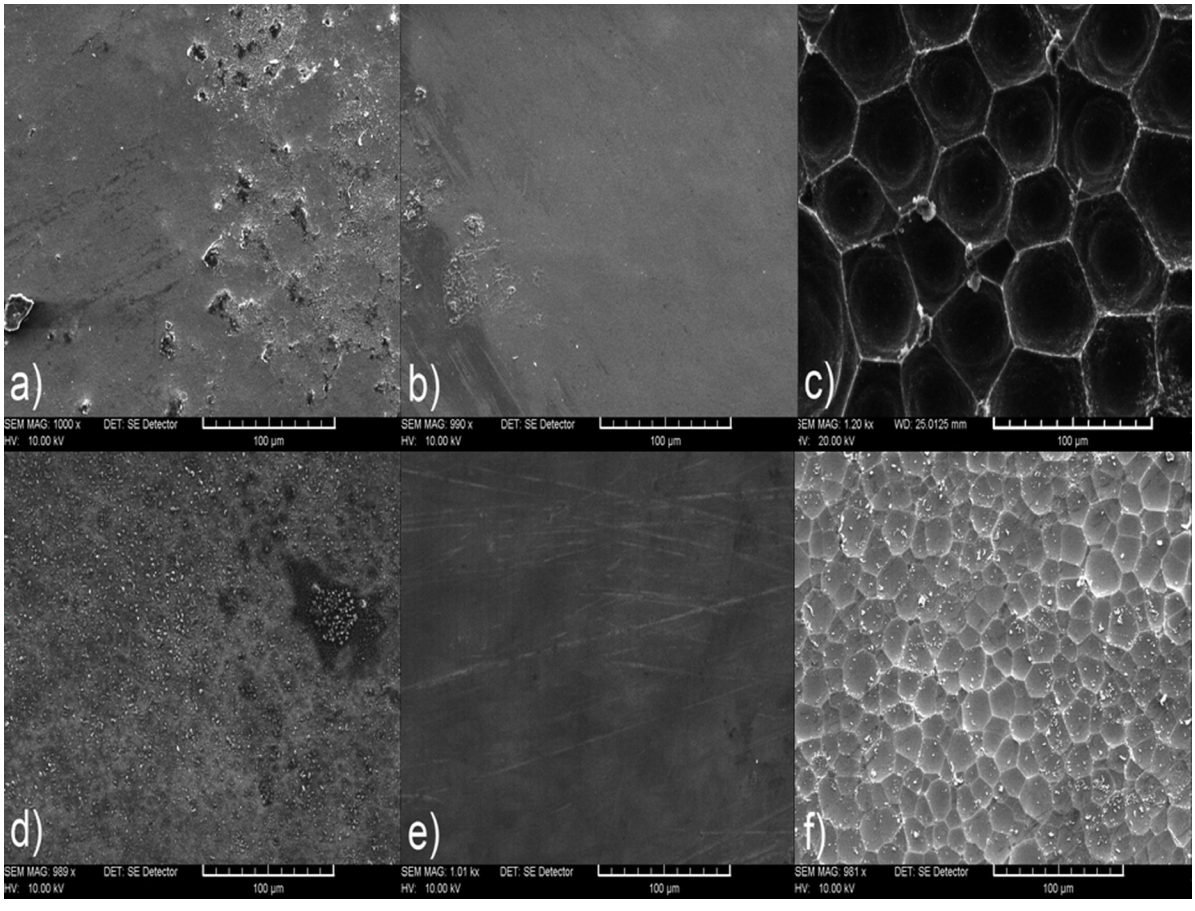


Fig. 3. SEM images of etched silicon samples (monocrystalline). The notations a – f refer to the compositions depicted in the ternary phase diagram in Fig. 1, indicating a systematic morphology change of the silicon surface after etching. Etching rates: a) $r$ = 171 nm $s^{-1}$, b) $r$ = 201 nm $s^{-1}$, c) $r$ = 354 nm $s^{-1}$, d) $r$ = 34 nm $s^{-1}$, e) $r$ = 119 nm $s^{-1}$ and f) $r$ = 135 nm $s^{-1}$.

a, d, and e). The "etching structures" in Figs. 3 a and 3 d as well as in the left part of Fig. 3 b may be induced by surface impurities.

The influence of a higher etching solution viscosity and possible protonation of HF molecules may bridle diffusion steps and thus the overall etching process. This is supported by data of Kolasinski who proposed the involvement of HF and $HF_2^-$ in the rate determining step for the mechanism of electrochemical silicon dissolution [24].

Higher water concentration reduces significantly the nitrosyl ion stability in the etching mixture by hydrolysis reactions and $HNO_2$ formation (Eq. 3). Nitrous acid disproportionates in the acidic etching solution (Eq. 4).

$$3\ HNO_2 \rightarrow HNO_3 + 2NO + H_2O \tag{4}$$

Consequently the silicon surface is not homogeneously covered with nitrosyl ions, but with a variety of secondary products as oxidizing agents having different oxidation potentials (Eqs. 5 – 7).

$$2\ NO + 2\ H^+ + 2\ e^- \rightarrow N_2O + H_2O,\ E^\circ = 1.59\ V \tag{5}$$

$$2\ NO + 2\ H^+ + 2e^- \rightarrow H_2N_2O_2,\ E^\circ = 0.71\ V \tag{6}$$

$$2\ HNO_2 + 4\ H^+ + 4\ e^- \rightarrow N_2O + 3\ H_2O,\ E^\circ = 1.29\ V \tag{7}$$

The surface reaction becomes much more region dependent and the silicon surface sites are not uniformly attacked. This leads to different vertical and lateral etching rates and to the formation of deep etching pits. The fact that these pits have a square/rectangular to hexagonal shape suggests that the novel etching mixture can be used for anisotropic structuring of

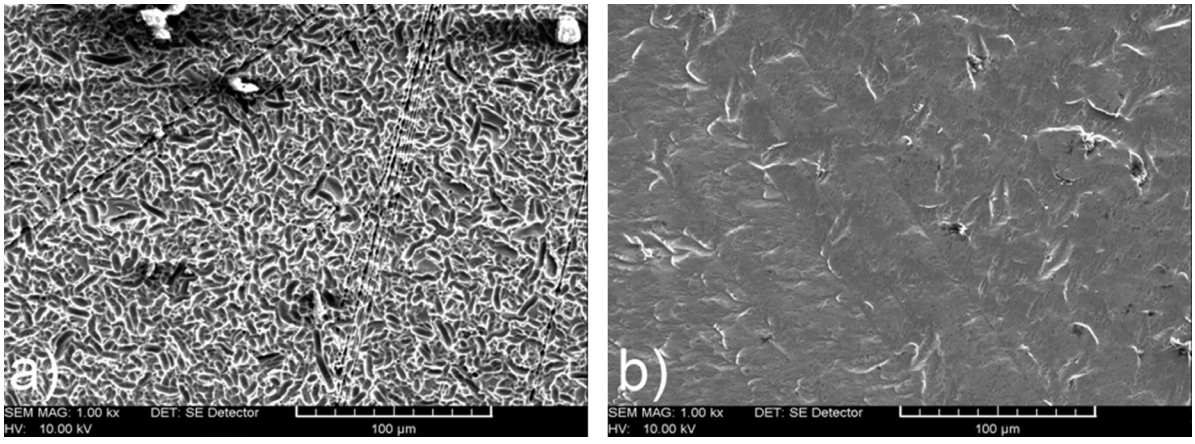


Fig. 4. SEM images of multicrystalline silicon surface morphologies after etching in: a) HF (6.36 mol $L^{-1}$) – $HNO_3$ (6.00 mol $L^{-1}$) – $H_2O$ (isotexture, $r$ = 164 nm $s^{-1}$); b) HF (6.36 mol $L^{-1}$, 13 wt %) – $NOHSO_4$ (6.00 mol $L^{-1}$, 32 wt %) – $H_2SO_4$ (55 wt %) (planarized, $r$ = 137 nm $s^{-1}$). For classification of the mixture composition see Fig. 1.

monocrystalline silicon wafers – a novelty for acidic etching solutions and so far only possible with alkaline etching solutions (NaOH, KOH) at high temperatures ($> 60$ °C). The geometry of the etch pits may reflect the $\langle 100 \rangle$ silicon surface superstructure. This effect is unexpected for acidic solution etching of $\langle 100 \rangle$ oriented polished silicon surfaces.

The higher stability of nitrosyl ions in concentrated acid solution gives rise to isotropic (polished) etching structures, whilst a high water content leads to formation of anisotropic etching structures (etch pits). In principle, with the novel etching mixture isotropic or anisotropic surface morphologies can be selectively produced.

The complex interactions of a variety of effects, *e. g.* local heating, masking of surface positions by gas bubbles, or side reactions of the nitrosyl ions with water and/or reduction products, make an unambiguous assignment of the resulting morphologies difficult. Further studies regarding the correlation between mixture composition and reactivity as well as etching surface morphology will provide more detailed information.

For comparison, two etched multicrystalline silicon surfaces, which were produced with equimolar parts of HF in a) HF – $HNO_3$ – $H_2O$ and b) HF – $NOHSO_4$ – $H_2SO_4$ mixtures are shown in Fig. 4. The well-known isotexture with visible grain boundary attacks (Fig. 4a) is characteristic for wafer processing with nitric acid based mixtures. In contrast, a floe-like silicon surface structure with very small etch pits is produced by the novel etching solution (Fig. 4b). The fact that the grain boundaries are not preferentially attacked qualifies the novel etching system as highly isotropic.

Likewise, rounded wafer morphologies are achievable by isotropic etching solutions consisting of HF – $HNO_3$ – $H_2SO_4$ or $HNO_3$ – $NH_4F$ – $H_2SO_4$ mixtures [25].

A characteristic effect of the novel etching mixtures is the observed dependence of the resulting silicon wafer morphology on the etching time. At the beginning of the etching process highly textured silicon surfaces are produced. After several etching turns with the same solution, planarized silicon surfaces arise (Fig. 5).

This remarkable result may be interpreted as a switch-over of the rate determining step due to consumption of reactive species of the etching system. An influence of local heating caused by the fast etching reaction cannot be ruled out. Since the nitrosyl ion concentration is high, the HF diffusion may become more rate determining with increasing reaction time. This is in full agreement with the observed morphologies. As a consequence, the silicon surface ablation decreases and polishing of the surface prevails after five etching turns.

*Analytical investigation of the silicon surface after the etching process*

The etched silicon surface was investigated by DR/FT-IR spectroscopy. Fig. 6 indicates $Si(–H)_x$ ($x$ = 1 – 3) termination, which has been proposed and con-

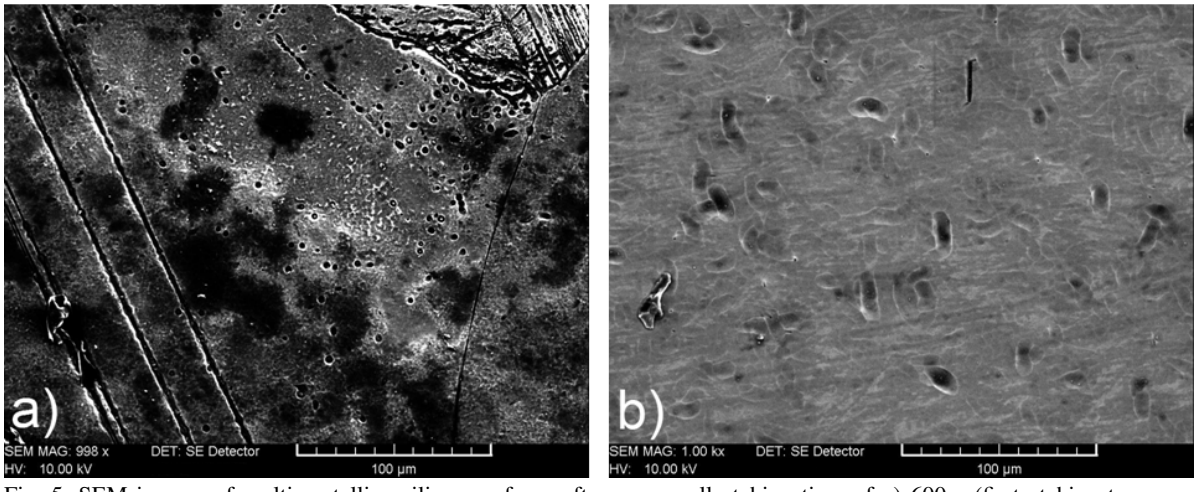


Fig. 5. SEM images of multicrystalline silicon surfaces after an overall etching time of a) 600 s (first etching turn, $r$ = 60 nm $s^{-1}$) and b) 3000 s (fifth etching turn, $r$ = 43 nm $s^{-1}$) in HF (7.45 mol/l, 20 wt %) – $NOHSO_4$ (2.05 mol $L^{-1}$, 14 wt %) – $H_2SO_4$ (66 wt %). For classification of the mixture composition see Fig. 1.

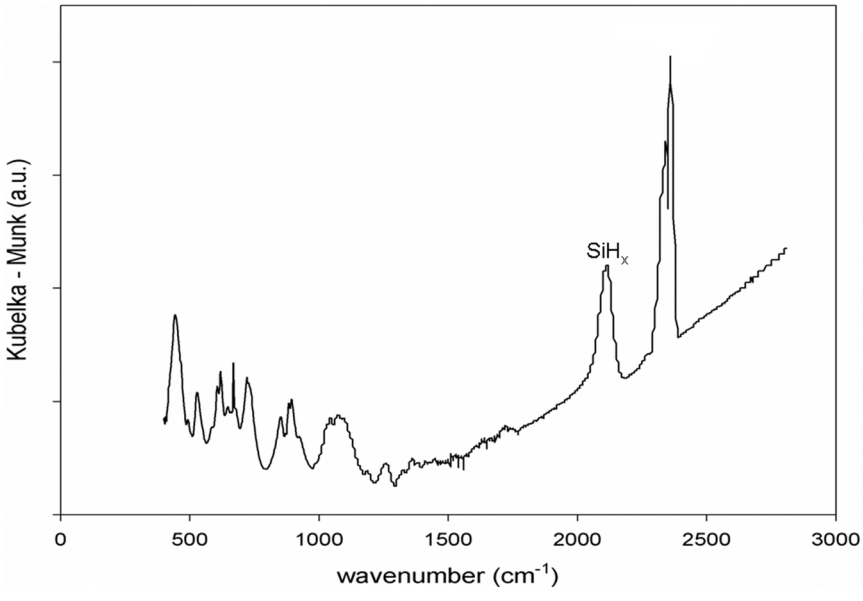


Fig. 6. DR/FT-IR spectrum of a silicon surface etched with the novel etching mixture. The intensive peak at 2360 $cm^{-1}$ can be assigned to $CO_2$ of the ambient air.

firmed experimentally for some isotropic etching processes [26, 27].

Because of the broadness of the $Si(–H)_2$ absorption band (2112 $cm^{-1}$), the presence of Si(–H) and $Si(–H)_3$ groups cannot be ruled out. In principle, the microscopic roughness of the multi-crystalline silicon surface should grant the formation of all $Si(–H)_x$ ($x$ = 1 – 3) surface species. The stability of the Si–H bonds in the highly acidic etching solutions is astonishing, especially considering the ($H^+$ + $H^-$) synproportionation reaction which should lead to the production of hydrogen. The final rinsing of the etched silicon samples with DI water at r. t. gives rise to slow attack of the hydrogen-terminated silicon surface by $H_2O$ and $O_2$ which leads to Si–O–Si, Si–O–H und O–Si–$Si(–H)_x$ groups [17, 28, 29]. Apparently the novel etching mixture follows the widely accepted oxidative addition reaction steps of HF molecules on crystalline silicon surfaces [26]. Investigation of the etching solutions has provided detailed insight into the process stages, the redox sequence of the oxidizing agent and the complexation of the oxidized surface silicon atoms.

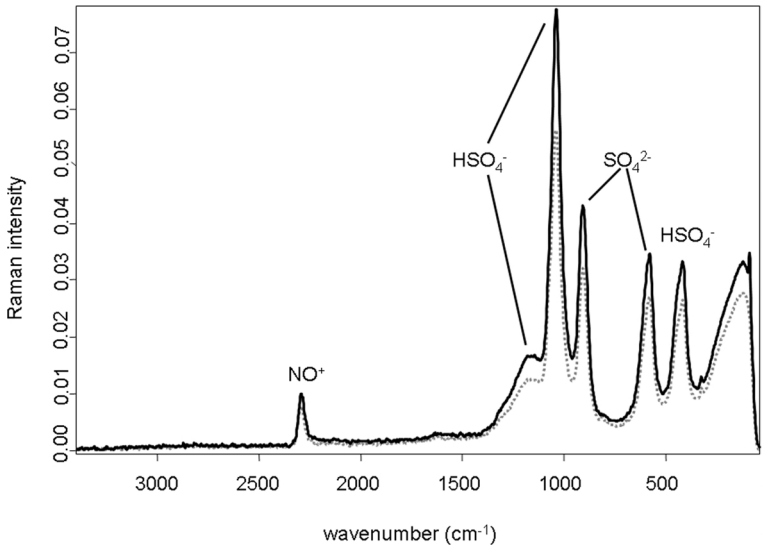


Fig. 7. Raman spectra of a HF – $NOHSO_4$ – $H_2SO_4$ mixture after different etching times. Graph a) (black) after 600 s and b) (grey) after 3000 s successive etching of 4 monocrystalline silicon wafer samples.

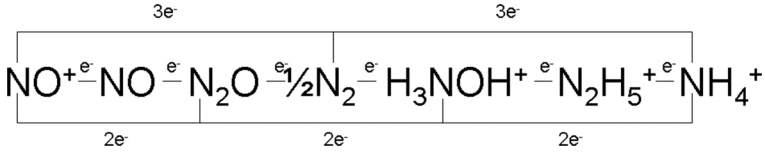


Fig. 8. Scheme of potential redox sequences for the oxidizing agent (nitrosyl ion).

*Investigation of the etching solution*

Due to characteristic absorptions of the etching mixture components ($NO^+$, $HSO_4^-$, $SO_4^{2-}$), Raman spectroscopy is the method of choice for fast analytical investigation (Fig. 7).

The Raman band at 2300 $cm^{-1}$ is unambiguously assigned to the stretching vibration of the nitrosyl ion. After 3000 s of etching ($r$ = 160 nm $s^{-1}$, $n_{Si}$(etched) = 0.003 mol) no dissolved nitrogen oxides, $NO_2$, NO or $N_2O_3$, are detected. The relative intensity of the stretching vibrations for the nitrosyl ion (2300 $cm^{-1}$) and the sulphate ion (900 $cm^{-1}$) remains constant. Thus, Raman spectroscopy appeared to be not sensitive enough for adequate nitrosyl ion quantification, but analysis of the etching solution by ion chromatography did indicate nitrosyl ion consumption by etching reactions.

The analysis of the used etching solution by $^{29}Si$ and $^{14}N$ NMR spectroscopy proved the complexation of oxidized silicon atoms as hexafluorosilicate ($SiF_6^{2-}$) and the reduction of the oxidizing agent ($NO^+$) beyond the oxidation state zero (molecular nitrogen $N_2$) to form ammonium ions ($NH_4^+$). No other reduction products were detectable so far in the etching solution.

Obviously, the reduction of the oxidizing agent does not stop at the stage of nitrogen monoxide (NO) as observed for conventional etching mixtures. This result points to a complex silicon oxidation mechanism, which possibly includes electrochemical and (photo)chemical oxidation steps. The exceptional reduction of $NO^+$ (+3) to $NH_4^+$ (−3) indicates a new reaction pathway for nitrogen-oxygen compounds in highly acidic solutions. This surprising result raises the question: Which consecutive steps are directly involved in the silicon oxidation sequence (Fig. 8)?

It is likely that $NH_4^+$ is produced as a by-product by disproportionation of nitrosyl ion reduction intermediates like hydroxylammonium ions (Eq. 8).

$$3\,[NH_3OH]^+ \rightarrow NH_4^+ + N_2O + 2\,H_3O^+ + H_2 \quad (8)$$

Due to the fact that several volatile products can be formed in the etching of silicon, the characterization of the gas phase contributes to an understanding of the overall etching reaction, in particular the relevant reduction steps of the oxidizing agent.

*Investigation of the gas phase*

During the etching experiments of crystalline silicon nearly colorless gases are observed. This stands

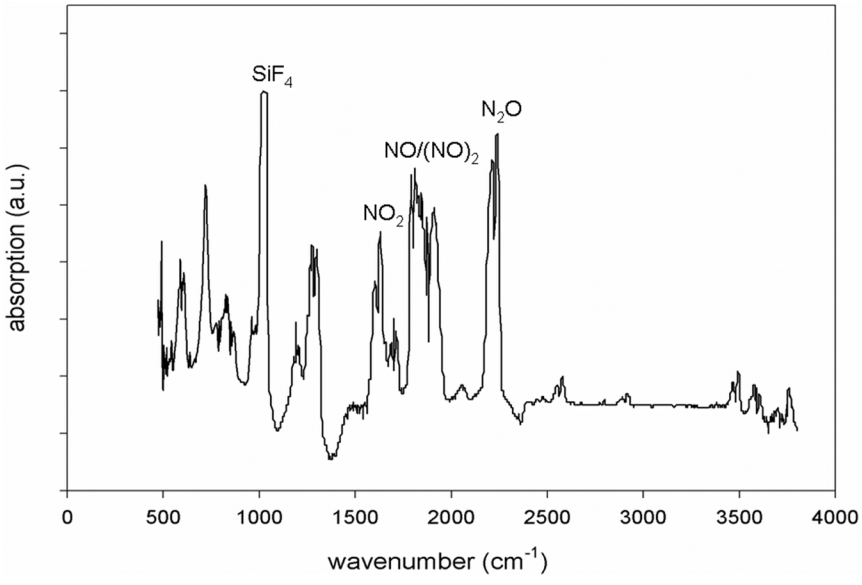


Fig. 9. FT-IR absorption spectrum of gaseous products for etching reactions with novel etching mixtures.

as a major difference to the intensively brown gas atmosphere resulting for etching with nitric acid based mixtures. The investigation by means of FT-IR spectroscopy proved the massive formation of $SiF_4$, $N_2O$, NO and $NO_2$ (Fig. 9).

The assignment of the remaining IR bands is not yet complete [30]. As indicated by NMR spectroscopy data, the oxidizing agent is reduced much further than just to NO. Recently, Weinreich has detected traces of $N_2O$ in the gas phase of the conventional etching system Si/HF – $HNO_3$ – $H_2O$ [31]. For the novel etching system $N_2O$ and especially $SiF_4$ are the main gaseous products; $NO_2$ is formed by secondary oxidation of NO with oxygen. Silicon tetrafluoride escapes from the etching solution evading $SiF_6^{2-}$ complexation.

Due to the IR-inactivity of their vibrational modes, $H_2$ or $N_2$ could not be identified in the IR study. However, preliminary Raman spectroscopic investigations of the gas phase indicated $H_2$ formation. NOF and $H_{4-x}SiF_x$ ($x = 1-3$) are probably present in very small concentrations, but were not positively identified. In order to propose a valid reaction mechanism, further investigations of the etching solution, the gas phase and the chemical as well as the physical nature of the silicon surface are essential.

*The influence of $Ag^+$ ions on the etching process*

The reactivity of the novel etching mixtures towards crystalline silicon as well as the surface morphology can be controlled by the addition of metal ions, for example $Ag^+$. The enhancement of the etching rate (reactivity) and the change of the wafer morphology towards that of polished silicon surfaces are illustrated in Fig. 10.

The etching process is probably stimulated by a facilitation of the electron transfer from the surface silicon atoms to the oxidizing agent by the aid of the silver ions. The azaphilic nature of the $Ag^+$ ions and the oxophilicity of the silicon atoms are likely to support establishing $Ag^{+\cdots}NO^{+\cdots}Si(H_x)$–$Si_{bulk}$ electron transfer bridges.

Except for the precipitation of elementary silver on the etched silicon wafers, there are no further differences between the reaction products of a stimulated and a silver-free etching process. Obviously, the silver ions react with the silicon surface by a catalytic interplay of the redox-pairs $Ag^+$/Ag/Si and $NO^+$/reduction products. Thus, the overall etching process is catalyzed by breaking the hydrogen passivation of silicon, which is known to be crucial for the attack of crystalline silicon by wet chemical etchants (Eq. 9) [26].

$$\begin{aligned} &=Si_{surf}(-H)_2 + 2\,Ag^+ + 2\,F^- \\ &\quad\rightarrow =Si_{surf}(H)(F) + HF + 2\,Ag\downarrow \end{aligned} \tag{9}$$

Consequently, the reactivity of hydrogen-rich surface positions, like steps and kinks (surface defects), is enhanced and these sites are etched preferentially, resulting in the observed "polishing" of the silicon surface. A

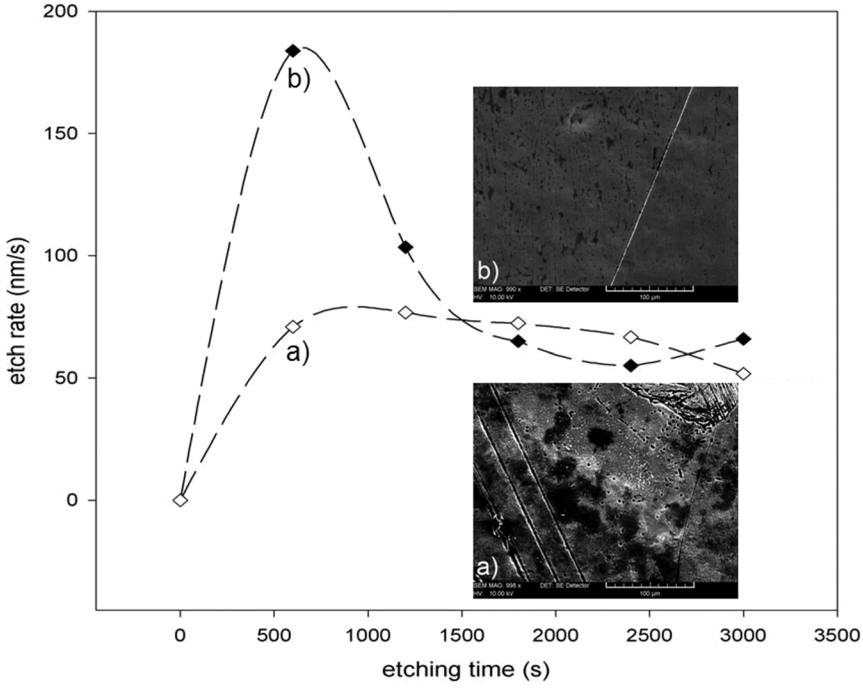


Fig. 10. Traces of silver ions (0.03 mol $L^{-1}$ $Ag^+$) have a strong impact on the silicon etching process: Novel etching mixture a) without silver ion and b) with silver ion addition. The insets show SEM images of multicrystalline silicon surfaces after the first etching turn. Scale bar length = 100 $\mu$m.

number of related studies were dedicated to electroless metal deposition (EMD) and electroless silicon etching. Peng used HF/$AgNO_3$ solutions for the formation of aligned silicon nanowires (SiNW) [32]. Ag nanoparticles are deposited onto the silicon surface of the substrate and catalyze the etching reaction. The particles sink below the surface and leave behind silicon nanostructures. Tsujino used HF – $H_2O_2$ – $H_2O$ mixtures to effectively texturize silicon surfaces by metal assisted electroless etching [33, 34].

We conclude that the metal-assisted ($Ag^+$/Ag) polishing of crystalline silicon surfaces with HF – $NOHSO_4$ – $H_2SO_4$ mixtures is based on a related mechanism. The formation of Ag particles on the silicon surface (Eq. 9) represents the initiating step. Like in the photographic process, more $Ag^+$ ions are attracted to the silver particles where they are reduced. Thus, the Si/Ag interface acts as a microcathode for reducing the oxidizing agent catalyzing the overall etching process. The formation of polished silicon surfaces in our new process is probably a consequence of the much higher Ag deposition rate.

## Conclusions

Novel etching mixtures based on nitrosyl salt solutions open up a new way for wet chemical etching of crystalline silicon. By a variation of the concentration ratios the silicon surface quality can be selectively controlled (texturing/polishing). For monocrystalline silicon this improved controllability is of particular relevance. The novel etching system is able to produce selectively isotropic or anisotropic surface morphologies. Silver salt addition gives rise to etching process stimulation.

The oxidation capacity is much greater for the Si/HF – $NOHSO_4$ – $H_2SO_4$ system than for conventional HF – $HNO_3$ – $H_2O$ mixtures, considering the reduction of the nitrosyl ions to $N_2O$ and $NH_4^+$. The diminished evolution of toxic nitrogen oxides contributes to cost saving by lower demands for exhaust gas treatment. Furthermore, owing to the massive $SiF_4$ formation, the used etching solutions are less contaminated with reaction products, beneficial with regard to the etching solution lifetime and consequently economically and ecologically advantageous for the semiconductor and photovoltaic industry, respectively.

## Experimental Section

*Preparation of the etching system HF – $NO^+HSO_4$ – $H_2SO_4$*

*Caution:* All manipulations were performed in an HF-proof hood. The concentrations of the solutions are given in weight percent (wt%) in reference to concentrated acids.

Analytical grade sulphuric acid (97 %, 18.78 mol $L^{-1}$), hydrofluoric acid (40 %, 22.77 mol $L^{-1}$) and deionized water (DI) were used for the etching solutions. The total volume of a typical etching solution was 50 mL. For a given solution, 40 % HF (10 wt %) means that the used etching solution contains 10 weight percent of 40 % hydrofluoric acid.

$NOHSO_4$ was synthesized by bubbling dried $SO_2$ into $HNO_3$ (100 %) for several hours [35].

The etching solutions were prepared by mixing the components in a HDPE beaker (high-density polyethylene). The temperature was kept constant during the series of experiments (RT = 20 °C) using a thermostat (Julabo ECF-12).

*Silicon materials and etching procedure*

The multicrystalline silicon wafers (boron doped, thickness 330 $\mu$m, resistivity 0.5 – 2 $\Omega\,cm^{-1}$, Deutsche Solar AG, Freiberg) and monocrystalline silicon wafers ($\langle 100 \rangle$ orientation, boron doped, thickness 625 $\mu$m, resistivity 75 – 95 $\Omega\,cm^{-1}$, Wacker Siltronic, Freiberg) respectively, were broken and after weighing immersed in the etching solution for exactly 600 s. The solution was agitated with a magnetic stirrer (200 r.p.m.). All reactions were quenched by removing the silicon wafer pieces out of the bath with a pair of teflon tweezers and rinsing them with DI water. The samples were dried and etching rates (nm $s^{-1}$) determined by differential weighing.

*Stimulation of the etching process by addition of $Ag_2SO_4$*

Silver sulphate was synthesized by conversion of silver nitrate ($AgNO_3$) with sulphuric acid. 0.09 g $Ag_2SO_4$ (3 mmol) were dissolved in the etching solution resulting in an $Ag^+$ concentration of 0.03 mol $L^{-1}$.

*Spectroscopic characterization of etching mixtures, the gas phase and the silicon surface*

The Raman spectra of the etching solutions were registered with a Bruker RFS 100/S instrument. The samples were excited by 1064 nm radiation of an Nd:YAG laser. The laser power was 200 mW, the scattered light was collected in 180° backscattering geometry and detected by a nitrogen cooled Ge detector.

The IR spectra of the gas phase and the silicon wafer surfaces were obtained using a Nicolet 510-FTIR spectrometer in transmission and by diffusive reflection (DR). The NMR spectra were registered using a Bruker DPX 400 spectrometer and teflon inserts. The resonance frequencies and reference standards for the $^{14}N$ and $^{29}Si$ nuclei were $NO_2CH_3$ (29 MHz) and $(CH_3)_4Si$ (79 MHz), respectively.

Surface morphology studies of etched silicon wafers were carried out with a scanning electron microscope VEGA TESCAN TS 5130 SB (10 kV, WD = 23 mm).


[1] P. Woditsch, W. Koch, *Solar Energy Materials & Solar Cells* **2002**, *72*, 11 – 26.
[2] G. Wenski, G. Hohl, P. Storck, I. Crössmann, *Chem. Zeit* **2003**, *37*, 198 – 208.
[3] O. Schmidt, N. Jin-Phillipp, *Appl. Phys. Lett*. **2001**, *78*, 3310 – 3312.
[4] H. Robbins, B. Schwartz, *J. Electrochem. Soc*. **1959**, *106*, 505 – 508.
[5] E. Abel, H. Schmid, *Z. Phys. Chem., Stoechiom. Verwandtschaftsl*. **1928**, *132*, 55 – 77.
[6] E. Abel, H. Schmid, *Z. Phys. Chem., Stoechiom. Verwandtschaftsl*. **1928** *134*, 279 – 301.
[7] D. Klein, D. D'Stefan, *J. Electrochem. Soc*. **1962**, *109*, 37 – 42.
[8] H. Schmid, H. Spahn, *Z. Metallkunde* **1955**, *46 (2)*, 128 – 137.
[9] K. Vetter, *Z. Physik. Chem*. **1950**, *194*, 199 – 206.
[10] M. Steinert, J. Acker, A. Henßge, K. Wetzig, *J. Electrochem. Soc*. **2006**, *152*, C843–C850.
[11] H. Robbins, B. Schwartz, *J. Electrochem. Soc*. **1960**, *107*, 108 – 111.
[12] B. Schwartz, H. Robbins, *J. Electrochem. Soc*. **1961**, *108*, 365 – 372.
[13] B. Schwartz, H. Robbins, *J. Electrochem. Soc*. **1976**, *123*, 1903 – 1909.
[14] G. Pietsch, Y. Chabal, G. Higashi, *Surf. Sci*. **1995**, 395 – 401.
[15] G. Pietsch, G. Higashi, Y. Chabal, *Appl. Phys. Lett*. **1994**, *64*, 3115 – 3117.
[16] G. Pietsch, Y. Chabal, G. Higashi, *J. Appl. Phys*. **1995**, *78*, 1650 – 1658.
[17] G. Pietsch, *Appl. Phys. A* **1995**, *60*, 347 – 363.
[18] S. Holt, P. Reynolds, J. White, *Phys. Chem. Chem. Phys*. **2000**, *2*, 5667 – 5671.
[19] T. Arai, D. Aoki, M. Fujihira, *Thin Sol. Films* **1996**, *273*, 322 – 326.
[20] I. Röver, G. Roewer, K. Bohmhammel, K. Wambach, *Proceedings of the 19$^{th}$ EPSEC*, Paris, **2004**, 895 – 898.
[21] M. Kelly, J. Chun, A. Bocarsly, *Appl. Phys. Lett*. **1994**, *64 (13)*, 1693 – 1695.
[22] A. Hantzsch, K. Berger, *Z. Anorg. Allg. Chem*. **1930**, *190*, 321 – 336.
[23] A. Bard, R. Parsons, J. Jordan, *Standard Potentials in Aqueous Solution*, Marcel Dekker, New York, **1985**.
[24] K. Kolasinski, *Phys. Chem. Chem. Phys*. **2003**, *5 (6)*, 1270 – 1278.
[25] C.-H. Du, M.-H. Hsieh, S.-Y. Tsai, *Proceedings of the 20$^{th}$ EPSEC*, Barcelona, **2005**, 1313 – 1316.

[26] H. Ubara, T. Imura, A. Hiraki, *Solid State Commun.* **1984**, *7*, 673 – 675.
[27] G. Trucks, K. Raghavachari, G. Higashi, Y. Chabal, *Phys. Rev. Lett.* **1990**, *4*, 504 – 507.
[28] G. Socrates, *Infrared and Raman Characteristic Group Frequencies. Tables and Charts*, Wiley, Chichester, **2001**.
[29] X. Sun, S. Wang, N. Wong, D. Ma, S. Lee, *Inorg. Chem.* **2003**, *42*, 2398 – 2404.
[30] F. Melen, M. Herman, *J. Phys. Chem.* **1992**, *4*, 831 – 881.
[31] W. Weinreich, Diploma Thesis, Freiberg University of Mining and Technology, Freiberg, Germany, **2005**.
[32] K. Peng, J. Hu, Y. Yan, Y. Wu, H. Fang, Y. Xu, S. Lee, J. Zhu, *Adv. Funct. Mater.* **2006**, *16*, 387 – 394.
[33] K. Tsujino, M. Matsumura, Y. Nishimoto, *Solar Energy Materials & Solar Cells* **2006**, *90*, 100 – 110.
[34] K. Tsujino, M. Matsumura, *Adv. Mater.* **2005**, *17*, 1045 – 1047.
[35] W. Schroeder, P. Urone, *Environ. Sci. Technol.* **1978**, *12*, 545 – 550.